Bull Volcanol (2010) 72:1169–1178
DOI 10.1007/s00445-010-0392-5

RESEARCH ARTICLE

Numerical model of crater lake eruptions

M. Morrissey · G. Gisler · R. Weaver · M. Gittings

Received: 17 June 2009 / Accepted: 6 July 2010 / Published online: 1 August 2010

Abstract We present results from a numerical investigation of subaqueous eruptions involving superheated steam released through a lake mimicking the volcanic setting at Mt. Ruapehu. The simulations were conducted using an adaptive mesh, multi-material, hydrodynamics code with thermal conduction SAGE, (Simple Adaptive Grid Eulerian). Parameters investigated include eruption pressure, lake level and mass of superheated vapor. The simulations produced a spectrum of eruption styles from vapor cavities to radial jets that resulted in hazards that ranged from small-scale waves to high amplitude surges that reached and cascaded over the edge of the crater rim. There was an overall tendency for lake surface activity to increase (including wave amplitude) with increasing mass of superheated vapor and eruption pressure. Surface waves were induced by the formation and collapse of a gas cavity. The collapse of the cavity is considered to play a major role in the characteristic features observed during a subaqueous eruption. The additional mass of superheated vapor produced a larger cavity that displaced a larger area of the lake surface resulting in fast moving surges upon the collapse of the cavity. High lake levels (>90 m) appear to suppress the development of explosive jetting activity when eruption pressures are <10 MPa. At very large eruption pressures (>10 MPa), vertical jets and radial ejections of steam and water can occur in water depths >90 m. Less explosive eruption styles can produce hazardous events such as lahars by the outward movement of surface waves over the crater rim.

Keywords Phreatic eruptions · Subaqueous eruptions · Numerical model · Crater lakes

Editorial responsibility: J. Phillips

M. Morrissey (✉)
Colorado School of Mines,
Department of Geology
and Geological Engineering,
1500 Illinois,
Golden, CO 80401, USA
e-mail: mmorriss@mines.edu

G. Gisler
University of Oslo, Physics of Geological Processes,
Oslo, Norway

R. Weaver · M. Gittings
Los Alamos National Laboratory,
Los Alamos, NM, USA

Introduction

Over the past decade, there have been a number of crater lake eruptions that resulted in catastrophic surface waves, dramatic changes in lake levels that sent flood water over crater rims producing devastating lahars and floods, or changes in lake chemistry (Fazlullin et al. 2000; Manville et al. 2000; Lecointre et al. 2004; Colvin et al. 2008). The onset of the 1995 eruptions at Mt Ruapehu volcano in New Zealand generated lahars from the explosions through the crater lake as it has done prior to major eruptions since 1861 (Fig. 1a; Ruapehu Surveillance Group 1996). The 1980 crater lake explosions at Mt. Ruapehu were characterized by a range of phenomena from black spear-head slugs ejected >1 km above the water surface, similar to explosions observed during emergence of an erupting submarine volcano, to geyser-like jets surrounded by a white, base-surge ring (Fig. 1b-c; Smithsonian Institute 2009). Similar phenomena were observed during the 1996 subaqueous eruption at Akademii Nauk volcano in Kamchatka (Fazlullin et al. 2000). Intermittent bursts of dark ash and lacustrine deposits and dome-shaped bubbles

Fig. 1 Photos of eruptive activity at Mt. Ruapehu in 1980, show black tephra jets, geyser-like vertical jets surrounding an outward moving surge, and lahars flowing down the flank of the volcano (SI 2009)

200–300 m in diameter occurred above the lake surface. Similarly, large bubbles (>10 m in diameter) were observed during the July, 1991 eruption in Lake Voui at Aoba volcano, Vanuatu (Bulletin of the Global Volcanism Network 1991) as well as at Karmskoye lake in Kamchatka during the 1996 eruption that included black jets of tephra and vapor (Belousov and Belousova 2001). Geyser-like eruptions were also observed at Akademii Nauk volcano and were accompanied by surface waves several meters high (Fazlullin et al. 2000). Flooding of the Karymsky River resulted from the series of subaqueous explosions and surface wave activity at Akademii Nauk volcano. An ecological hazard developed from shock waves generated from subaqueous explosions that rapidly changed the lake water composition killing as many as 300,000 fish during the eruption (Fazlullin et al. 2000).

A recent compilation of volcanic hazards revealed that only 8% of all recorded eruptions occurred through lakes and seawater yet this small fraction of volcanic activity caused 20% of all recorded fatalities (Mastin and Witter 2000). Of all hazards associated with eruptions through crater lakes and seawater, lahars caused most fatalities followed by pyroclastic flows, tsunamis and other surface waves, and base surges (Mastin and Witter 2000). This raises the question: under what conditions are these various hazards produced? To address this question, we apply a numerical model SAGE (SAIC Adaptive Grid Eulerian) that is capable of modeling subaqueous environments. SAGE was developed at Science Applications International Corporation (SAIC) and Los Alamos National Laboratory to study underwater explosions in shallow water and the effects of ocean depth, ocean bottom materials, and depth of burst on the resulting shock waves at various depths and ranges. We adapt SAGE to simulate the crater lake environment at Mt Ruapehu and the 1995 eruptive events observed and recorded on a monitoring network

(RSG 1996). Results from hydrodynamic simulations of subaqueous phreatic eruptions (Barberi et al. 1992) are used to estimate the physical (water depth, crater lake diameter) and initial thermodynamic (temperature, pressure, water to steam mass-ratio) conditions that generate the various phenomena and hazards observed during crater-lake eruptions such as Mt. Ruapehu.

Model

Background

Numerical investigations of subaqueous volcanic eruptions have been limited to thermodynamic models that either calculate eruption energies and velocities for compressible fluids ranging from pure steam to hot rock and water mixtures (Mastin 1995) or simulate the effect of adding water to a one-dimensional eruption column (Koyaguchi and Woods 1996; Mastin 1997). These models demonstrate that when the mass fraction of water is slightly increased and the mass flux of magma that produces a Strombolian type of an eruption stays the same, the result is an increase in eruption energy and in plume height, and deposits that are considered dry due to the conversion of water to steam (Mastin 1995; Koyaguchi and Woods 1996). With increasing mass fraction of water to the system, the result is a wet, dense and cool eruption column that collapses onto a flow of wet ash (Mastin 1995; Koyaguchi and Woods 1996). These earlier models demonstrate the effects of water on eruption column thermodynamics, but do not address the effects of the fluid dynamic processes involved with mixing of multiple fluids and eruption processes.

Some aspects of the dynamic behavior of shallow (on the order of less than tens of meters) underwater explosions have been identified though experimental studies involving high explosive chemical detonations (e.g., Kedrinskii 2005). These experiments are viewed in this paper as first order analogs of subaqueous volcanic eruptions thus providing valuable insight into the fluid dynamic processes related to the response of water to an explosive discharge. The general phenomena observed in the experiments were the development of a vapor cavity, the upheaval of the free surface of the water due to the rise of the cavity, the collapse of the cavity and the vertical throw of water (Fig. 2a). There are two experiments that are most applicable to subaqueous volcanic eruptions, one is from the use of a bubbly medium (Zimanowski et al. 1997) and the other relates to the depth of the detonation (Kedrinskii 2005, p. 346). When a bubbly mixture was used as opposed to a uniform liquid, the results included the formation of radial jets or streamer structures that appeared to behave similarly to denotation experiments using soil producing a Surtseyan-like eruption (Fig. 2b; Kedrinskii 2005). The streamer structures result from instabilities that form under expansion of a cavitating liquid layer (Kedrinskii 2005). For a homogenous liquid, an explosion at very shallow depths produces a vertical jet structure or sultan from the inertial motion of the free surface immediately above the expanding vapor cavity. As the depth of detonation or explosion increases, in addition to the initial jet or sultan, a subsequent rebound jet forms that later reverses direction to produce a cumulative jet extending above the free surface (Kedrinskii 2005). As the explosion depth increases, the initial sultan ceases to form and only the secondary or cumulative jet forms. The initial conditions for these experiments are not completely reported therefore we report the phenomena without bounding conditions.

To further our understanding of subaqueous volcanic eruptions, we utilize a hydrodynamic code SAGE developed at SAIC and Los Alamos National Laboratory to study highly turbulent flows. The code is a multiphase, hydrodynamic and compressible fluid dynamic code that includes heat transfer. For such problems that require a high-resolution grid and long distances and time spans, a continuous adaptive mesh-refining (CAMR) algorithm is used that dynamically refines the zone size of the mesh at each spatial point and each time step during the calculation. The CAMR allows cells to be subdivided into smaller cells where steep gradients in flow properties occur and recombined to larger cell sizes when gradients are small.

Numerical model SAGE

As mentioned earlier, SAGE is a multi-dimensional, multi-material, Eulerian hydrodynamics code for use in solving the conservations equations for mass, momentum and energy in a variety of high-deformation flow problems. SAGE is designed to calculate flow and thermodynamic parameters as functions of space and time therefore each material region is initialized not only by its thermodynamic state (pressure and temperature, or density and temperature or internal energy) but also by flow properties such as velocity. These parameters are calculated through out the simulation and may be analyzed in animation form or as snapshots of the computational domain.

The computational domain of SAGE may be 1-dimensional, 2-dimensional or 3-dimensional defined by initial conditions of the fluid dynamic and thermodynamic state of each material phase (i.e., H_2O gas or H_2O liquid). Each material phase defines a region of the domain by location and shape. For instance, in the case of defining a conduit filled with H_2O gas, the shape would be a cylinder with a specified radius and length, filled with H_2O gas. The wall regions may be defined as rigid reflectors or solid material with strength. SAGE has a tensor-like artificial viscosity that eliminates the development of discontinuities during the calculation. Details on the

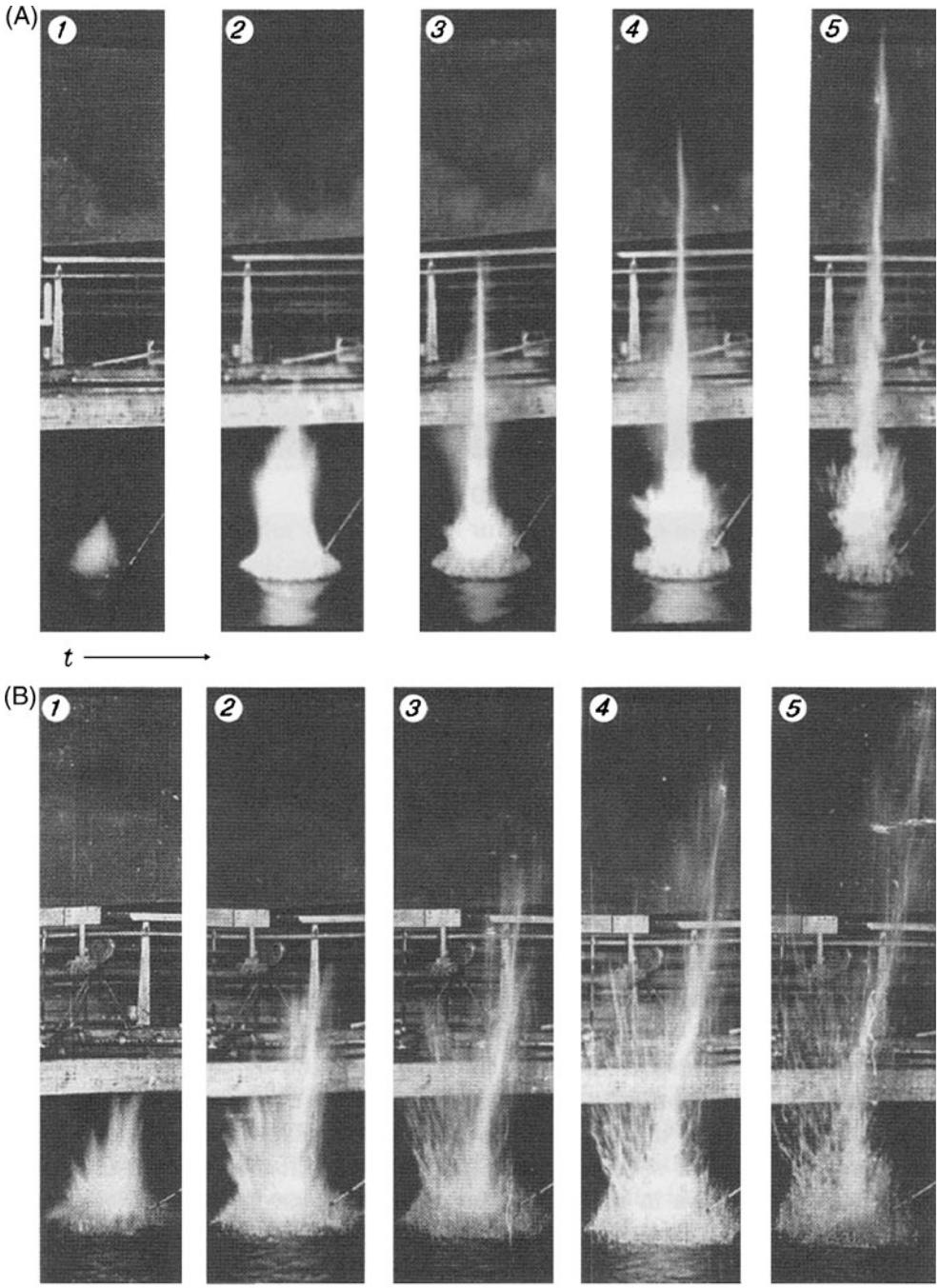

Fig. 2 Underwater explosion experiments designed to study hydrodynamic processes. **a** Experiment that produced a vertical jet (sultan), and (**b**) one that produced streamers or radial jets (Kedrinskii 2005)

physics and algorithms in SAGE as well as the verification and validation may be found in Gittings et al. (2008).

SAGE utilizes sophisticated forms of the equation of state (EoS) for water and other materials. The EoS for all materials are either in the form of tables in terms of $v_m(P, T)$ and e_m (P, T), where v_m is the specific volume, P is pressure, T is temperature, and e_m the specific energy of a specified material m or in SESAME form which is converted to tabular form. The SESAME EoS form is a standardized, computer-based library of tables for the thermodynamic properties of materials developed and maintained by the Mechanics of Materials and EoS Group of the Theoretical Division at Los Alamos National Laboratory; more detail may be found at http://t1web.lanl.gov/newweb_dir/t1sesame.html. SAGE assumes that all cells are mixed zones thus containing more than one material that are in pressure and temperature equilibrium. This assumption allows for a multi-material equation of state to be described by the total volume and energy. The EoS for water is in SEASAME form that accurately

describes water in all phases from ice to supercritical making SAGE an appropriate model for studying subaqueous eruptions.

Application

Computational set-up

The purpose of the simulations is to define the initial conditions that produce a certain subaqueous volcanic eruption style ranging from passive surface waves to explosive jets. A range of eruption styles have been observed at the crater lake at Mt. Ruapehu in 1980 and 1995 and the lake conditions have been monitored for decades (i.e. Dibble 1974; Christenson 1994; Sherburn et al. 1998; Branan 2008), making it suitable for comparison to models with SAGE. The computational domain (Fig. 3) mimics the profile of the crater lake at Mt. Ruapehu constrained from Christenson (Fig. 8; 1994) that includes vent location and diameter, crater wall slopes and crater diameter. The vertical distance from lake bottom to the crater rim is 140 m. The crater lake geometry is assumed radial for purposes of making the calculation 2-dimensional with cylindrical symmetry. Below the vent is the conduit defined as a cylinder with a diameter of 50 m using the conceptual model derived by Christenson (1994). The length of the conduit is assumed to be >1 km. For modeling purposes, we consider the upper several hundred meters of the conduit with the lower boundary defined by constant flow conditions. The crater and conduit walls are assumed rigid, non-elastic medium and thermally conductive.

The fluid phases involved in the simulations include air, H_2O and andesitic melt. The initial 1995 eruptions at Mt. Ruapehu erupted through the crater lake ejected very little juvenile material. The absences of juvenile or fragmented magma suggests that the early phases of the eruption involved mostly magmatic volatiles trapped in the upper conduit that released once the internal pressure exceeded the tensile strength of the cap rock (RSG 1996; Self et al. 1979). Most explosive eruptions are primarily driven by the volumetric expansion of high-pressure magmatic volatiles (mostly H_2O) to atmospheric conditions resulting in the conversion of internal energy to mechanical energy (Kieffer 1989; Mastin 1995). We assume H_2O as the dominant magmatic volatile involved in the 1995 Mt. Ruapehu crater lake eruptions with an initial temperature of at least 975°C. The upper portion of the conduit is filled with superheated H_2O vapor and the lower portion is filled with andesitic magma. Andesite in the simulations is defined as an incompressible fluid and given a very low velocity (relative to decompressing gas) to simulate a slow moving degassed magma. The mass of the vapor phase is treated as a variable in the simulations whereas the mass of andesitic magma remains the same in each simulation. The atmosphere is air at thermodynamic conditions for the appropriate elevation. The crater lake is assumed to contain pure water, the presence of additional chemical elements is neglected. The level of the crater lake at the onset of the 1995 eruption was 120 m from the bottom that we consider full without breaching the crater rim.

Investigated parameters

A series of calculations in two dimensions with cylindrical symmetry are conducted to study the interaction of a gas eruption through a crater lake and the surface waves generated in the crater lake. The parameters that are investigated include: water depth, mass of superheated vapor, and initial pressure of erupting superheated vapor. Table 1 lists the values selected for the three parameters in each calculation. Two lake levels are considered either the crater-lake was full (120 m) or the water depth is 90 m. The mass of superheated vapor is defined by the upper conduit length and initial pressure. The upper conduit length ranged from 60 m to 300 m with the most of calculations using 200 m (Table 1). The initial pressure of superheated vapor inside the conduit ranged from 0.5 MPa to 15 MPa. We use

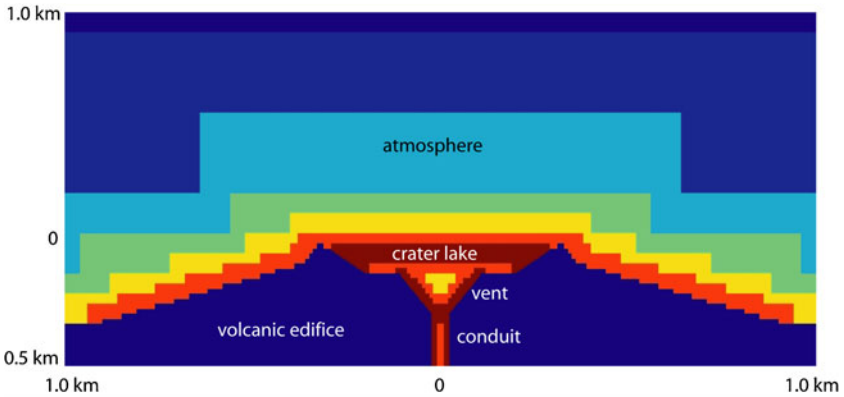

Fig. 3 Example of the initial computational domain of crater lake simulation C1. Colors denote grid cell size in units of meters. Distance from rim to upper conduit at the bottom of the crater lake is 140 m. Crater rim radius is 280 m and the conduit radius is 25 m

Table 1 List of parameters and values investigated for each calculation. R denotes the mass ratio of the lake water to superheated vapor. Superscript *v* denotes length of the upper conduit occupied by superheated vapor. Characteristic features of resulting simulated eruption activity are included in table

	C1	C2	C3	C4	C5	C6	C7
Lake depth (m)	120	120	120	90	90	90	120
Pressure (MPa)	5	10	10	10	5	0.5	15
Conduit^{v} length (m)	200	200	300	200	200	60	200
Vapor mass (10^6 kg)	3	7	10	7	3	0.1	10
R	3170	1580	1060	490	980	3270	1060
Max Jet Height (m)	0	100	180	80	60	0	185
Jet Type	None	Vertical	Vertical	Radial	Vertical	none	Radial
Wave Size	Small surface disturbances	10 m surges	20 m surges	10–20 m surges	<5 m surges	Small surface disturbances	20–30 m surges
Crater Rim Breached	No	Yes	Yes	Yes	No	No	Yes

the term eruption pressure to refer to the pressure of fluid at in the upper conduit at the onset of the simulation or the initial pressure of fluid in the upper conduit. The vent of the conduit is located at the base on the lake from which at the onset of the calculation superheated vapor is instantaneously released into the lake. The range of pressure and conduit length values yielded a mass for superheated vapor that ranged between ~10^5 kg to ~10^7 kg. The initial mass of lake water involved in the calculations was either 10^{10} kg (full) or 3×10^9 kg (half-full). We consider the entire mass of lake water and not the mass of the water column above the vent because, as the results will demonstrate, the entire lake is involved in the interaction with the erupting magmatic fluid as defined by the term R, the mass ratio of lake water to superheated vapor. R is quantified by the initial masses of lake water and superheated vapor for each calculation.

Results

The series of calculations resulted in a spectrum of activity that ranged from small-scale surface waves to a series of surge waves accompanying radial jets. The style of activity depended on eruption pressure, the initial mass ratio of lake water to superheated vapor and lake level as illustrated in Fig. 4. As illustrated in Fig. 5, calculations involving $R>$ 1100, a full lake and superheated vapor with an initial pressure between 0.5 MPa and 5.0 MPa produced a vapor cavity that raised the lake surface several meters before it collapsed or cavitated causing small disturbances on the lake surface within <25 sec. At eruption pressures between 5 MPa and 10 MPa, and R between 1100 and 1600 (Fig. 4), the vapor cavity rose through the lake displacing the lake surface tens of meters before it began to collapse (Fig. 6a). As the cavity collapsed (Fig. 6b), a vertical jet formed reaching a height of 100–200 m above the crater-lake surface. As the lake surface dropped due to the collapse of the vapor cavity, surge waves formed along the base of the jet (Fig. 6c). The surges were several meters high and move rapidly toward the rim of the crater lake eventually cascading over the edge. The surges are composed of saturated steam due to turbulence of the lake surface. At vapor pressures >10 MPa (Fig. 4) with R <1600 in a full lake, the vapor cavity rose rapidly through the lake, expanding the lake surface radially >100 m to a point where instabilities formed producing fingers or streamers of liquid (Fig. 7a-b). The upward momentum of the interior of the expanding cavity decreased resulting in its collapse and the initiation of a vertical jet. The initial displacement of the lake surface produced a series of surges 10 s m high that moved toward the crater rim and cascaded over the walls. The time scale of the simulations is on the order of seconds; the observed fluid dynamic events occur within 10–20 sec.

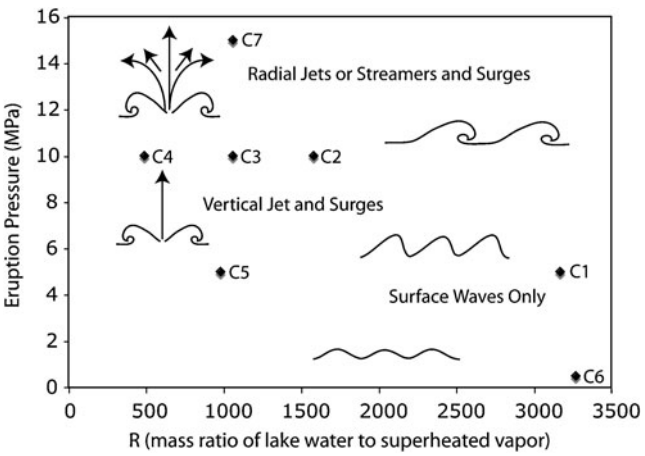

Fig. 4 Summary of simulated activity associated with noted calculations as a function of R and eruption pressure

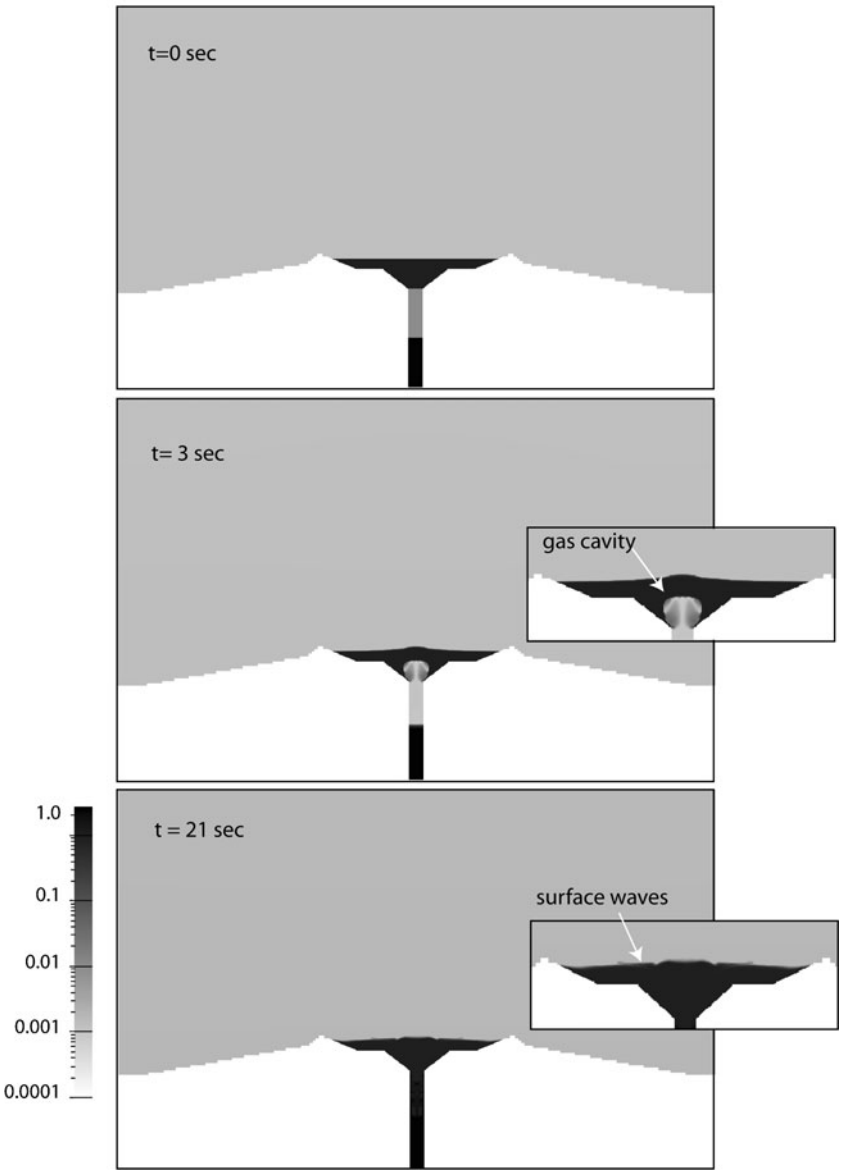

Fig. 5 Snapshots of the density field from simulation C1 (see Table 1) showing surface waves produced from the collapse of the gas cavity. Insets show details of fluid dynamics inside gas cavity. Grey log-scale represents density in units of kg/m^3. Wall rock is not part of the grey scale value scheme

The effect of lake level (included in R) on the eruption style for similar eruption pressures and mass of superheated vapor is demonstrated upon comparing results from calculation 1 (C1) with calculation 5 (C5), and calculation 2 (C2) with calculation 4 (C4) in Table 1. For the same initial conditions, a half-full (90 m) lake favored a more energetic ejection of vapor into the lake then a full lake as observed by the increase in expansion of the cavity through the lake (Figs. 5 and 6). When the lake was full (120 m), higher eruption pressures and additional mass of superheated vapor were necessary to achieve similar activity in the lake relative to when the lake was half full.

In each simulation, a vapor cavity developed that initiated the fluid dynamic processes that produced the range of simulated eruption activity. The cavity is initiated by the ejection of a vertical column of superheated vapor into the bottom of the lake and the rapid development of a vortex at the water-superheat vapor interface (Fig. 5). The working surface of the vortex expands radially forming the classic mushroom structure entraining cooler vapor from the boundary with the lake water. At high values of R ($\geq$1060) and low eruption pressures (<0.5 MPa), the initial mass of superheated vapor is limited and from which only a small vapor cavity can form. The growing convecting cavity eventually loses sufficient heat to the lake and is unable to sustain its growth resulting in cavitation (Fig. 6). At this stage, lake water flows into the conduit previously occupied by vapor. At lower values of R (<1060), the collapse of the vapor cavity results in lake water circulating down into the area previously occupied by the vapor cavity

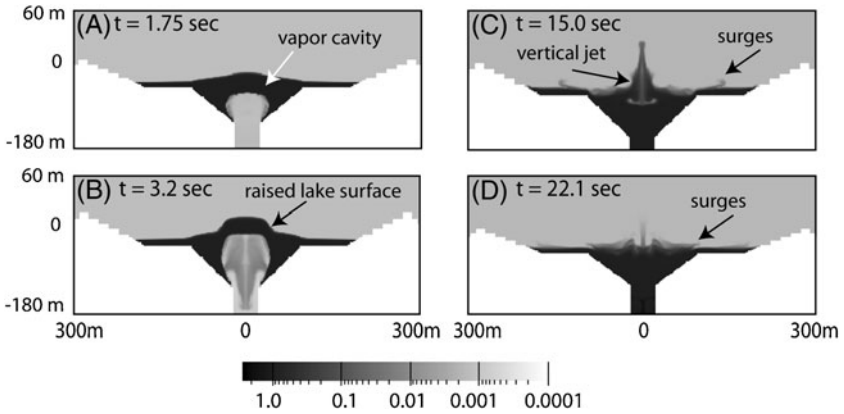

Fig. 6 Snapshots of the density field from simulation C5 (see Table 1) showing the gas cavity raising the lake surface 14 m before cavity collapses generating initial surge waves and a jet that later collapses forming a complex series of surges. Snapshots show only a small area of the total computational domain (Fig. 3). Grey log-scale represents density in units of kg/m^3. Wall rock is not part of the grey scale value scheme

in the vent and upper conduit (Fig. 5). The down flow of lake water produces an upwelling of a jet in the center of the lake producing geyser-like, vertical jets. At lower values of R (<1060) and higher eruption pressure (>0.5 MPa; Fig. 7), superheated vapor is ejected into the lake at velocities at or near its sound speed initiating a supersonic jet. As in the previous case, a vortex forms at the vapor-lake boundary forming a cavity of superheated vapor. The additional mass of superheated vapor from the conduit allows the jet to grow inside the cavity resulting in the rapid expansion of the upper vapor-lake boundary where Rayleigh-Taylor instabilities form. These instabilities develop into streamer-like structures upon the collapse of the cavity creating radial jets. Because of the turbulent boundary layers in the cavity and the fixed mass of superheated vapor, the cavity eventually collapses. Results from the simulations with eruption pressures >0.5 MPa, are similar in ejection patterns as observed at Mt. Ruapehu (Fig. 1).

Discussion

The simulations of discrete ejections of superheated vapor through a crater lake produced a spectrum of hazards from surfaces waves to radial jets and surges. The results suggest

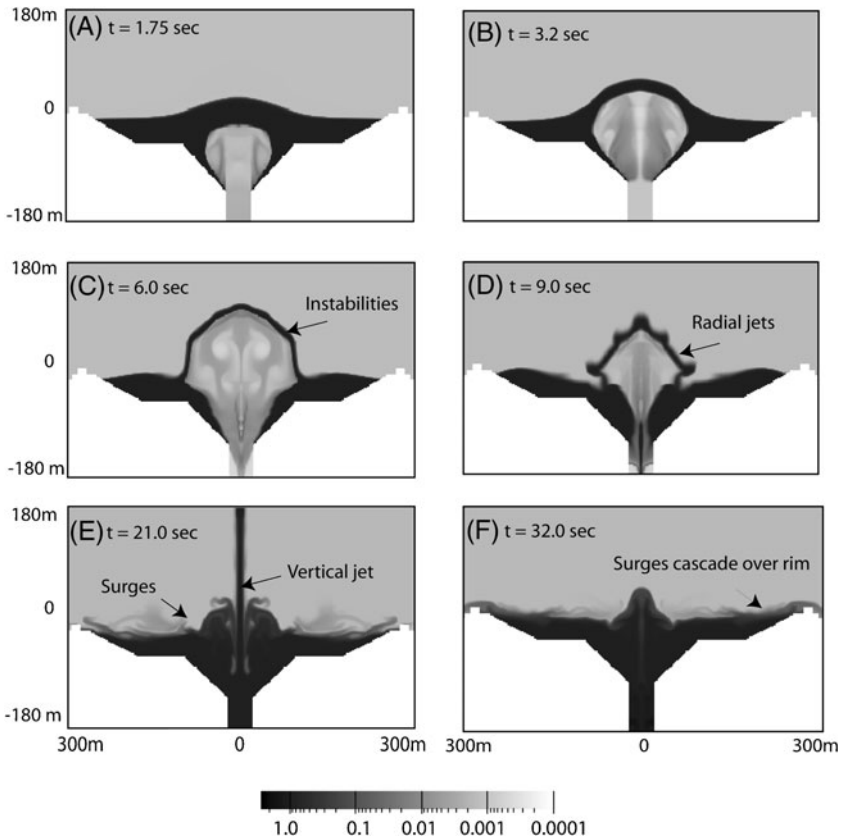

Fig. 7 Snapshots of the density field from simulation C3 (see Table 1). A gas cavity rapidly forms and expands raising the surface 90 m before collapsing. As the cavity collapses, instabilities form along the lake surface forming finger or radial jets that coincide with the development of the main vertical jet. Surge flows are observed to flow toward the crater rim where they eventually cascade over the rim and begin to flow down the crater walls. Snapshots show only a small area of the total computational domain (Fig. 3). Grey log-scale represents density in units of kg/m^3. Wall rock is not part of the grey scale value scheme

an overall tendency for lake surface activity to increase with increasing mass of superheated vapor and eruption pressure, and decreasing lake levels (Fig. 4). As R decreased, surface waves increased in amplitude and vertical jets developed. The additional mass of superheated vapor produced a larger vapor cavity that displaced a larger area of the lake surface resulting in larger surface waves that reached and cascaded over the crater rim walls. Larger eruption pressures enhanced the expansion rate and final volume of the vapor cavity for a fixed mass of superheated vapor resulting in the formation of instabilities along the expanding lake surface from which radial jets formed. This observation has implications for the fluid dynamic processes associated with Surtseyan eruptions that are characterized by tephra jets and base surges. The simulations involved purely superheated vapor expanding adiabatically into the lake, however, if a mixture of superheated vapor and fragmented melt were ejected in the lake, the presence of fragmented melt of a fine grain size (<0.1 mm) should enhance jetting activity due to isothermal expansion of lake water to vapor (Wohletz 1986). In general, the presence of magma provides additional thermal energy as well as a means of introducing fragmentation processes that may lead to more explosive products. The results presented here are reasonable for an eruptive phase that is gas-rich or involves a mixture of gas and finely fragmented (<0.1 mm) magma prior to interaction with lake water.

The formation of a superheated vapor cavity is a common feature in all simulations and has been observed at geysers (i.e., Keiffer 1989) and during subaqueous eruptions (i.e., Kokelaar 1986; Belousov and Belousova 2001). Analysis of tephra samples collected from the 1963 eruption at Surtsey volcano in Iceland has suggested that during the subaqueous eruptions at the Surtla vent some of the fragmenting magma was shielded from direct contact with water (Kokelaar and Durant 1983). A steam copula was proposed for explaining tephra grains that do not appear to have experienced water-magma interaction (Kokelaar and Durant 1983; Kokelaar 1986). A video recording of the 1996 eruption at Karmskoye Lake in Kamchatka (Belousov and Belousova 2001) revealed that 100–200 explosions occurred in the lake. The explosions were characterized by black jets of tephra, steam and water through a shell of water (Belousov and Belousova 2001). The shell of water that likely formed from a vapor bubble that displaced the lake surface and was perforated by the tephra jets. The collapse of a vapor cavity releases latent heat and a pressure wave that propagates into the conduit (Keiffer 1989). Resonance from bubble collapse or cavitation has been attributed to similar behavior during geyser eruptions (Keiffer 1989) and may explain the discrete, pulsating eruptive activity observed during Surtseyan eruptions. Vapor cavities or bubbles therefore appear to play an important role in subaqueous volcanic eruptions.

As demonstrated by the simulations, vapor cavities or steam copulas can indeed form underwater and would be expected to develop during subaqueous eruptions (i.e. Surtseyan). Vapor cavities do not always show a significant surface expression and are short-lived features. The source of superheated vapor may be exsolution from magma and/or trapped lake water (or sea water) heated indirectly by magma. For example, the exsolution of 1–3 wt.% H_2O from magma rising 200 m in a conduit similar to Mt. Ruapehu would release 10^6 kg of superheated H_2O. As magma rises to the surface it will release H_2O along with other gas phases; the initial eruption phases associated with basaltic and andesite magmas (i.e. Hawaiian and Strombolian eruptions) are known to be gas-rich (Vergniolle and Mangan 2000). Considering these styles of eruption through water rather than the atmosphere, discharging gases would create bubbles or cavities that vary in size reflecting the mass of gas. A gas-rich eruption would form a large gas cavity underwater such as that observed at Karmskoye Lake (Belousov and Belousova 2001). The release of a mixture of fragmented magma and gas through the gas cavity would expand and form a "dry" vapor-rich cavity without mixing with water until the cavity collapses and the expanding jet would likely entrain water. The cavitation of the cavity may also initiate turbulent interaction of water with magma at depths beneath the lake or sea surface. Such a scenario may explain many of the observations recorded during subaqueous eruptions and from deposits associated with subaqueous eruptions.

Conclusions

Numerical simulations of crater-lake eruptions were conducted using the computer code SAGE to investigate eruption parameters such as eruption pressure and mass of gas on eruption style and hazards. The crater-lake simulations produced a spectrum of eruption styles from vapor cavities to radial jets. These eruption styles produced corresponding hazards that were mainly surface waves that ranged from small-scale waves to high amplitude surges that reached and cascaded over the edge of the crater rim. There was an overall tendency for lake surface activity to increase (including wave amplitude) with increasing mass of superheated vapor and eruption pressure (Fig. 4). Surface waves were induced by the formation and collapse of a gas cavity. The additional mass of superheated vapor produced a larger cavity that displaced a larger area of the lake surface resulting in fast moving surges upon the collapse of the cavity. Under certain conditions, vertical and radial jets occurred in addition to surface waves. High lake levels (>90 m) appear to suppress the development of explosive jetting activity when eruption pressures are <10 MPa. At very large eruption pressures (>10 MPa), vertical jets and radial ejections of steam and water can occur in water

depths >90 m. Less explosive eruption styles can produce hazardous events such as lahars by the outward movement of surface waves over the crater rim.

The release of superheated vapor into a lake produces a gas cavity that expands and then collapses producing disturbances in the lake. The collapse of the cavity is considered to play a major role in the characteristic features observed during a subaqueous eruption. The collapse of the cavity is known to release latent heat and pressure waves (Keiffer 1989). The pressure waves may propagate and resonate inside a conduit that may be attributed to the discrete, pulsating nature of Surtseyan eruptions. This hypothesis will be investigated in future studies.

We conclude that explosive eruptions through a crater lake require a critical mass of superheated vapor and the formation and collapse of a gas cavity. For crater lakes with water depths >100 m, our results suggest that a minimum mass of superheat vapor of 10^6 kg and eruption pressure >5 MPa are required to produce explosive eruptions from the lake such as observed in 1995 at Mt. Ruapehu (Lecointre et al. 2004) and at Karmskoye Lake (Belousov and Belousova 2001). Eruption pressures <5 MPa would produce surface waves that range between passive, small amplitude waves to base surges that can reach the edge of the crater-lake and initiate lahars or flooding on the flanks of the volcano.

Acknowledgements This project was funded by the National Science Foundation through grant #EAR-9614228. We would like to thank Richard Wendlandt for his review of the manuscript.

References

Barberi F, Bertagnini A, Landi P, Principe C (1992) A review on phreatic eruptions and their precursors. J Volcanol Geotherm Res 52:231–246

Belousov A, Belousova M (2001) Eruptive process, effects and deposits of the 1996 and the ancient basaltic phreatomagmatic eruptions in Karymskoye lake, Kamchatka, Russia. In: White JDL, Riggs NR (eds) Volcaniclastic sedimentation in lacustrine settings. Blackwell Sciences, Oxford, pp 35–60

Branan N (2008) Tracking deadly lahars; a new dataset provides the best evidence yet for research hoping to learn how to predict these torrential mudflows. Geotimes 53:28–30

Bulletin of the Global Volcanism Network (BGVN) (1991) Caldera lake bubbling; burned vegetation, Vol. 16:07. Smithsonian Institute.

Christenson BW (1994) Convection and stratification in Ruapehu Crater Lake, New Zealand: implications for a Lake Nyos gas release eruption. Geochem J 28:185–197

Colvin S, Rose WI, Escobar D, Gutierrez E, Montalvo F, Olmos R, Palma J, Varekamp J, Patrick M (2008) Crater Lake Evolution During Volcanic Unrest: Case Study of the 2005 Phreatic Eruption of Santa Ana Volcano, El Salvador Eos Trans. *AGU, 89*(53), Fall Meet. Suppl., Abstract V44A-06.

Dibble RR (1974) Volcanic seismology and accompanying activity of Ruapehu volcano, New Zealand. In: Civetta L, Gasparini R, Luongo G, Rapolla A (eds) Physical volcanology. Elsevier, Amsterdam, pp 49–85

Fazlullin SM, Ushakov SV, Shuvalov RA, Aoki M, Nikolaeva AG, Lupikina EG (2000) The 1996 subaqueous eruption at Academii Nauk volcano (Kamchatka) and its effect on Karymsky lake. J Volcanol Geotherm Res 97:181–193

Gittings ML, Weaver RP, Clover M, Betlach T, Byrne N, Coker R, Dendy E, Hueckstaedt R, New K, Oakes WR, Ranta D, Stefan R (2008) The RAGE radiation hydrodynamic code. Comput Sci Disc 1(015005):63

Kedrinskii VK (2005) Hydrodynamics of explosions: experiments and models. Springer-Verlag, Berlin, p 362

Kieffer SW (1989) Geologic nozzles. Rev Geophys 27:3–38

Kokelaar BP (1986) Magma-water interactions in subaqueous and emergent basaltic volcanism. Bull Volcanol 48:275–289

Kokelaar BP, Durant GP (1983) The submarine eruption of Surtla (Surtsey, Iceland). J Volcanol Geotherm Res 19:239–246

Koyaguchi T, Woods AW (1996) On the formation of eruption columns following explosive mixing of magma and surface-water. J Geophys Res 101:5561–5574

Lecointre J, Hodgson K, Neall V, Cronin S (2004) Lahar-triggering mechanisms and hazard at Ruapehu Volcano, New Zealand. Nat Hazards 31:85–109

Manville V, Hodgson KA, Houghton BF, Keys JR, White JDL (2000) Tephra, snow and water: complex sedimentary response at an active snow capped stratovolcano, Ruapehu, New Zealand. Bull Volcanol 62:278–295

Mastin LG (1995) Thermodynamics of gas and steam-blast eruptions. Bull Volcanol 57:85–98

Mastin LG (1997) Evidence for water influx from a caldera lake during the explosive hydromagmatic eruption of 1790, Kilauea Volcano, Hawaii. J Geophys Res 102:20093–20109

Mastin LG, Witter JB (2000) The hazards of eruptions through lakes and seawater. J Volcanol Geotherm Res 97:195–214

Ruapehu Surveillance Group (RSG) (1996) Volcanic eruption at a New Zealand ski resort prompts reevaluation of hazards. Eos, Transactions, AGU 77:189

Self S, Wilson L, Nairn IA (1979) Vulcanian eruption mechanisms. Nature (London) 277:440–443

Sherburn S, Bryan CJ, Hurst AW, Latter JH, Scott BJ (1998) Seismicity of Ruapehu, New Zealand, 1971–1996: a review. J Volcanol Geotherm Res 88:255–278

Smithsonian Institute (SI) (2009) Types of Processes Gallery – Magma meets water. Global Volcanism Program. http://www.volcano.si.edu/world/tpgallery.cfm

Vergniolle S. Mangan M (2000) Hawaiian and Strombolian eruptions, in: *Encyclopedia of Volcanoes*. In: Sigurdsson H (ed). Academic Press, p 447.

Wohletz KH (1986) Explosive magma-water interactions: thermodynamics, explosion mechanisms, and field studies. Bull Volcanol 48:245–264

Zimanowski B, Büttner R, Lorenz V (1997) Premixing of magma and water in MFCI experiments. Bull Volcanol 58:491–495